Proceedings of the 9th U.S. National and 10th Canadian Conference on Earthquake Engineering
Compte Rendu de la 9ième Conférence Nationale Américaine et
10ième Conférence Canadienne de Génie Parasismique
July 25-29, 2010, Toronto, Ontario, Canada • Paper No 1185

SHAKING TABLE TESTING OF A POST-TENSIONED TENDON FRAME RETROFITTED WITH METALLIC SHEAR PANEL DISSIPATOR

M. Dietz[1], O. Oddbjornsson[1], M. Ojaghi[2],
C.A. Taylor[1], M.S. Williams[2], & A. Blakeborough[2]

ABSTRACT

Two alternative passive seismic protection technologies have been combined in a single experiment to assess their synergy. The first, a nonlinear-elastic post-tensioned tendon frame, uses steel tendons to connect structural elements. Joints can rotate elastically allowing large recoverable interstory sway. Such structures have limited energy dissipation capabilities but are able to re-centre themselves after a seismic event. The second, a metallic shear panel energy dissipator has a large energy dissipation capacity but, as it is unable to self-centre, may impart a residual sway or offset to a structure after a seismic event.

This paper presents a series shaking table tests conducted at ¼ scale to assess the coaction of these technologies under realistic seismic loading. Repeat testing is used to investigate the fatigue lifecycle. While challenging to perform, the tests reveal the technologies to be complementary, each contributing beneficial characteristics to the global response.

Introduction

In an effort to enhance the damage resilience of structures, the past 20 years have seen passive protection technologies gradually being incorporated into seismic design practice. Such technologies work to reduce the seismic demand placed on structural systems by modifying the stiffness or damping. One such technology uses post-tensioned tendons to create dry joints between structural elements that are capable of significant elastic rotations. These allow significant interstory sways without sustaining damage to the structural elements. Post-tensioned tendon structures have a number of favourable properties: a self-centring capacity, an elastic (albeit nonlinear) response, and resilience to damage. However, without provisional support mechanisms, high sway magnitudes can bring about tendon yield potentially bringing about the collapse of the structure. Additionally, the energy dissipation (and hence the sway reduction capability) inherent in such structures is small.

[1] Dept. of Civil Engineering, University of Bristol, UK.
[2] Dept. of Engineering Science, University of Oxford, UK.

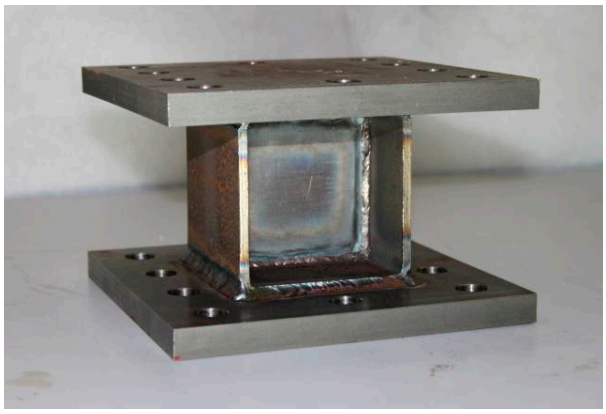

Figure 1. The device

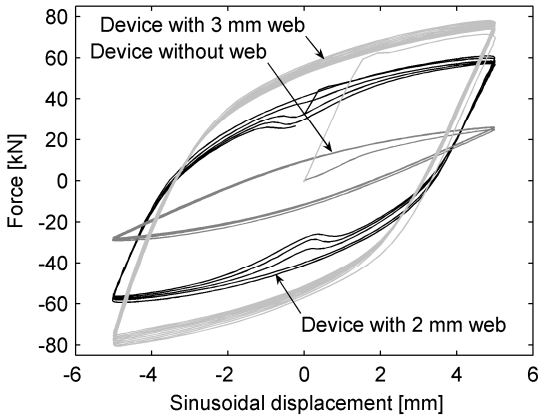

Figure 2. Constant strain amplitude response.

An alternative technology works to reduce interstory sway by absorbing seismic energy that would otherwise be imparted to the structure. The various types of dissipative device available can be classified by their mechanism of operation: viscous fluid, viscoelastic, friction or metallic (Soong & Dargush, 1997). The popularity of such devices stems from their versatility both in terms of installation locations and to their ability to be used in either new build or in existing structures as a retrofit. While such devices have large energy dissipation capacities they are unable to self-centre and may impart a residual offset to a structure after a seismic event.

The different approaches to structural damage reduction evident in the above mentioned technologies are potentially complementary. By limiting the sway, a dissipative device could prevent tendon yield in extreme earthquakes and reduce damage to non-structural components during design-basis earthquakes. By self-centring after an earthquake event, a post-tension tendon structure could remove any residual offset that would otherwise be imparted by a dissipative device. This work aims to make a preliminary assessment of the synergy of these technologies. A shaking table is used to test a ¼ scale model of a post-tensioned tendon frame (‘the frame’) retrofitted with a dissipative device (‘the device’) under realistic seismic loading. Comparisons are made with the pre-retrofit response of the frame to the same loading conditions and with the response of the device outside of the frame when subjected to constant strain amplitude sinusoidal tests.

Experimental setup

The device

The energy dissipation device used in this work is a mild steel shear-panel as pictured in Fig. 1. It is derived from a design originally proposed by Dorka at the University of Kassel, Germany, (Schmidt et al. 2004) and has been subject to testing and development elsewhere (Ojaghi et al. 2008).

The device is manufactured using 100mm lengths of structural steel (S355) box section (100x100x5mm) bounding a mild steel web welded centrally to resist shear. The box section is capped with top and bottom weld plates which are secured within the stiff chevron or shear wall bracing system of a structure. Unusually for a metallic device, energy is dissipated through shear yielding rather than bending. As a result, the device has the potential to offer high energy dissipation relative to the amount of material used and an improved fatigue resistance. However, like all metallic dissipative devices, this device is a sacrificial element requiring replacement after major seismic loading. While able to sustain repeated earthquakes, it does so with reducing effectiveness.

A series of constant strain amplitude sinusoidal tests were conducted at the Structural Dynamics Laboratory of the University of Oxford to assess this device's energy dissipation capabilities. Further details of the test rig can be found elsewhere (Ojaghi et al. 2008). Three examples of the device were tested: the first was fitted with a 3mm thick web; the second, a 2mm thick web; the third had no web at all. A 1Hz, 5mm relative displacement was applied across each device in turn. The resulting hysteresis loops are displayed in Fig. 2. The hysteresis loops for the webbed devices have substantial enclosed areas indicating a large energy dissipation capability. As the web thickness diminishes, so does the stiffness and the energy the device is able to dissipate.

Cyclical tests to failure conducted by Ojaghi et al. (2008) suggested that such devices have a three-tiered lifecycle. The opening stage is associated with maximum stiffness and dissipation and proceeds until an X shaped crack first become evident centrally within the web. During the second stage, the X crack expands into the corners of the web. The ultimate stage initiates when crack propagation ceases leaving only the box section intact and ends with box failure. Each successive stage in the device lifecycle is associated with diminished stiffness and dissipation.

The frame

Post-tensioned tendon structures were conceptualised in 1991 as a part of the University of California's PRESSS research program and realised using precast reinforced concrete frames (Priestly, 1991). Since that time, the technology has matured and design guidelines for such structures have been produced (Stanton & Nakaki, 2002). Additionally, the concept has been applied to other structural materials including steel (Garlock et al., 2005, Ricles et al., 2001) and timber (Newcombe et al., 2008), as well as to other structural types, most notably bridge columns (Palermo et al, 2005). However, the complexity associated with the dynamics of such structures has not yet been realised. Furthermore, how these dynamics can be controlled with the addition of dissipative devices has not been addressed.

The ¼ scale model of the post-tensioned tendon frame used in this work is depicted (with a device installed) in Figure 3a. It was designed in accordance with the guidelines noted above and was constructed as a part of a research program investigating the dynamic response of this class of structures (Oddbjornsson 2007, 2009). It employs the self centring frame concept in a single direction and, as such, is designed to be tested uniaxially in its long (y) direction (i.e. left to right in Fig. 3a).

(a)

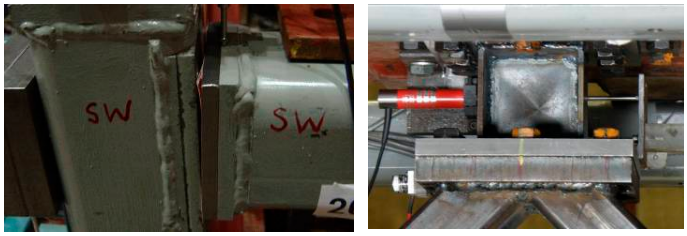

(b) (c)

Figure 3. Longsection of frame (a) and detail of a beam to column joint (b) and the device as installed within the frame (c)

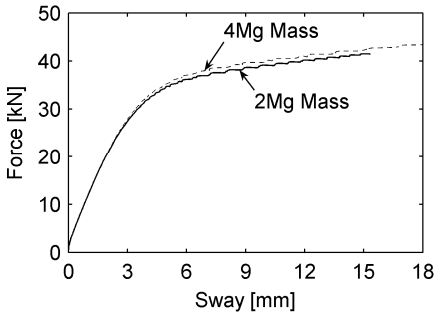

(a)

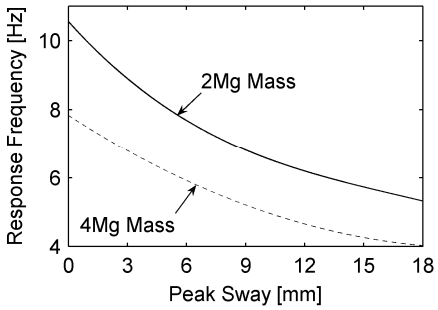

(b)

Figure 4. The frame's pushover curve (a) and frequency sway relationship (b).

The frame has a (c/c) beam length of 2.1m and a column height (to centre of the beam) of 0.9m. The base shear was determined according to the Direct Displacement Based Design method (Priestley, 2002) for a design drift of 20mm. With a 100x100mm joint contact area, the design guidelines suggest a tendon tension and cross section of 115kN and 93mm^2 for beam tendons and 64kN and 52mm^2 for column tendons. The beam and column elements were made from 100x100x10mm steel square hollow section, having 20mm thick endplates. The contact surface between elements is steel to steel. The material selected for the elements does not have significant influence on the generic behaviour of the system since the properties of the joints between elements define the system's global behaviour. A detail of an open beam to column joint is shown as Fig 3b.

The fundamental mechanics of the frame (with no device) were investigated using a series of pushover and free vibration (snapback) tests. As seen in Fig. 4a, pushover testing confirmed the nonlinear softening force-deflection characteristics of the model. Data from repeat tests fell on the same line, confirming the elasticity and the consistency of the response. The model's nonlinear dynamic stiffness was investigated by converting the time between zero crossings during free vibration tests into response frequency. The relationship between the response frequency and the peak sway is shown in Fig. 4b illustrating the frame's nonlinear dynamic stiffness. While the artificial mass simulation scaling procedure (Harris, 1999) requires a true ¼ scale model to have an active mass of 4Mg, tests were also conducted using a 2Mg active mass. The results in Figure 4 indicate the lower active mass to respond equivalently but with a frequency shift.

The test rig

Testing is conducted using the shaking table at the Bristol Laboratories for Advanced Dynamic Engineering (BLADE), the main facility for experimental research into earthquake engineering at the University of Bristol. The table consists of a 4Mg, 3m by 3m cast aluminium seismic platform capable of carrying a maximum payload of 15Mg. The platform is driven horizontally and vertically by eight 300mm stroke, 75kN servo hydraulic actuators. Hydraulic power for the actuators is provided by five pairs of hydraulic pumps capable of delivering 900 litre/min at a working pressure of 210bar. Platform motion is controlled in all six degrees of freedom simultaneously using PIDL architecture.

Preliminary testing revealed that both the scale and the dynamics of the self-centring frame would challenge the ability to control the shaking table. Uniaxial sine sweep testing (in the y direction) induced roll of the shaking table (i.e. about its x axis) at even low frequencies indicating that excessive overturning moments were being applied to the table. At higher frequencies, the self-centring frame began to sway and inertia forces were of sufficient magnitude to disrupt the shaking table and distort the input motion. An adaptive algorithm capable of updating the controller PIDL parameters in light of the changing frame dynamics would diminish these unwanted effects. However, implementation of such an algorithm was beyond the scope of this work. Instead, shaking table performance was enhanced by halving the active mass of the self-centring frame (from 4Mg to 2Mg) and doubling the table mass (by securing 4Mg dead load to the seismic platform). The modified model-to-table mass ratio allowed frame sways of 10-15mm to be induced without any significant distortions to the intended table motion. Table roll was negated. Note that a reduced active mass of 2Mg distorts the model similitude; the frame is no longer a true ¼ scale model. However, since the mechanics are unchanged (Fig. 4) the model retains its vital features and remains within the post-tension tendon class.

Testing

Additional modification was required to further enhance the compatibility of the experimental components once the frame was retrofitted. Early tests demonstrated that the shaking table was unable to generate sufficient inertia in the 2Mg active mass of the frame to shear a 2mm webbed device. A reduction in the stiffness of the device was required to facilitate the correct functioning of the system. This was achieved by reducing the device web thickness to 1mm.

Three test series were conducted: ‘F’, ‘D’ and ‘O’. During F series tests, the frame was tested in its pre-retrofitted state. D series tests featured the frame retrofitted with a 1mm web device. O series tests featured the frame with a modified device consisting of box section but no web. As depicted in Fig. 3a and c, the device was installed within the frame immediately below the active mass. The device weld plates were secured to the active mass above and to a chevron type bracing system below. The stiffness of the bracing system was as high as practicably possible in order to maximise shear displacement across the device. The shaking table test sequence involved successive applications of a seismic load. In this way, the fatigue life of the device was investigated. Individual tests will be referred to with a numeric appendage to the test reference so that, for example, the 4th test on the retrofitted frame is called D4.

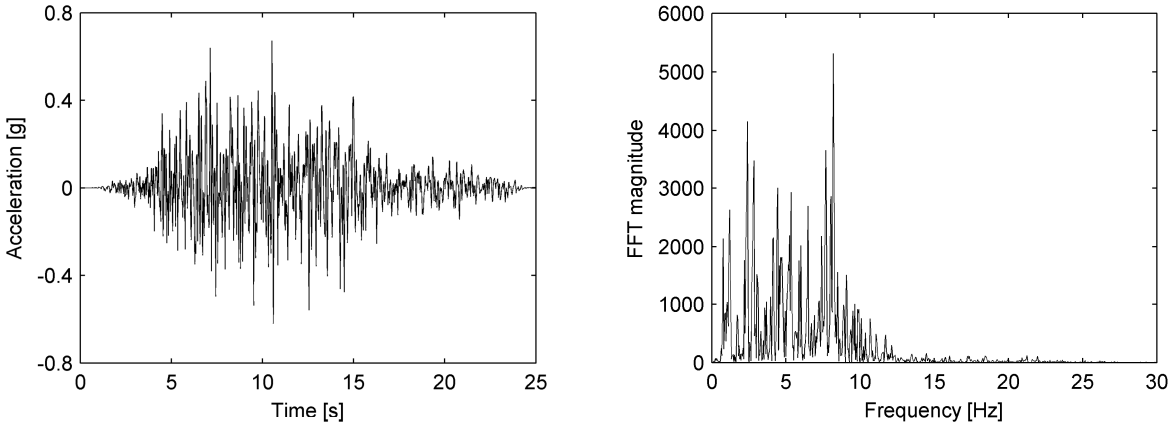

(a) (b)

Figure 5. The Loma Prieta earthquake in the (a) time and (b) frequency domain.

The experimental system was instrumented with accelerometers, load cells, strain gauges and linear displacement sensors. The results presented herein take the form of accelerations and sways. The 'excitation' and 'response' accelerations were recorded in the direction of shaking (y) on the shaking table and the active mass respectively. The sway is the relative horizontal displacement in the direction of shaking (y) between the active mass and the shaking table. Note that the horizontal displacement between the device weld plates was also recorded and found to be within 0.2mm of the sway. An initial test series was used to assess the resonant characteristics of the experimental system. A random signal (white noise) of bandwidth 1-50Hz was used to excite the shaking table in the y-direction giving root-mean-square accelerations of 0.1g. Frequency response functions (FRFs) were calculated by normalizing the response acceleration by the excitation acceleration in the frequency domain. The resonant frequencies for the frame pre and post retrofit were found to be 8.8 and 27Hz respectively.

The Loma Prieta earthquake recorded in the EW direction at the Waho station (Fig. 5) was selected as the seismic load due to its large energy content at around the natural frequency of the frame. With the frame in place, an iterative procedure was used to reproduce this time history in the required (y) direction while minimising parasitic motions in the 5 other degrees of freedom. In this way the shaking table performance was optimised.

Test results and discussion

Ojaghi et al. (2008) show that during constant strain level tests device lifespan decreases with strain magnitude and argue that large amplitude tests 'may exaggerate the real loading that must be absorbed by the device'. The variable strain amplitude seismic tests conducted for this work seem to support this statement. The devices used during both D series and O series tests demonstrate a remarkable seismic resilience. Test series D contains 18 seismic events. It is not until Test D10 that X cracks appear at the centre of the web, and not until Test D18 that these cracks propagate to the web corners. Test series O contains 27 individual seismic events. During Test O27 cracks propagated through the box section leaving the upper weld plate of the device detached from the lower.

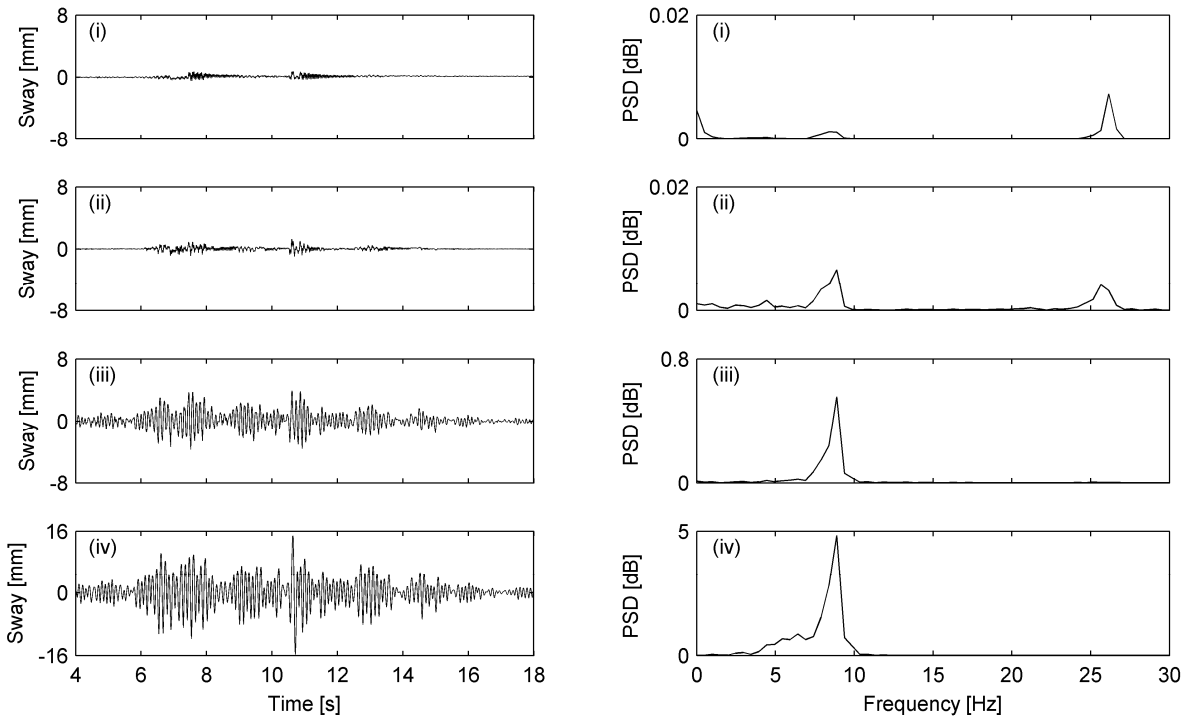

Figure 6. Response in terms of (a) interstory sway and (b) power spectral density for (i) Test D1, (ii) Test D4, (iii) Test O1 and (iv) Test F1.

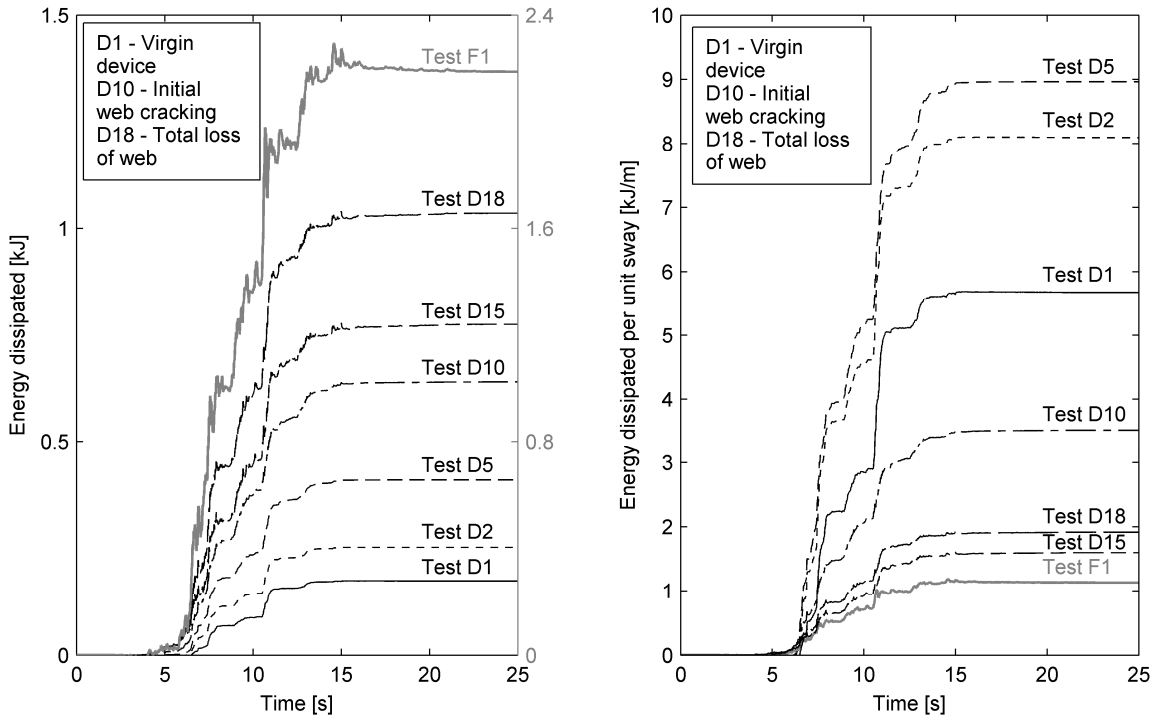

Figure 7. Energy dissipated (a) and energy dissipated per unit sway (b) during select tests.

The sway response of typical D, O and F series tests is contrasted in Fig. 6. During Test D1, the high stiffness of the virgin device keeps sway small. The small sways that do occur are predominantly at 27Hz, the system resonant frequency as determined from white noise testing. As the earthquake number increases two effects become apparent: firstly, peak sways increase; second, the power-spectral-density peak at 27Hz diminishes and is replaced by a peak at 8Hz. By Test D17, the 8Hz sways achieve a magnitude similar to those recorded during Test O1. However, sways remain an order of magnitude lower than those exhibited during Test F1. It is clear that the device is effective in reducing sway. Moreover, the resilience of the device suggests an ability to reduce sway during a main earthquake event and any subsequent aftershocks. However, the data thus far presented does not reveal whether the device is working as an energy dissipater or whether the reductions in sway are merely a result of increased stiffness.

Energy dissipation

The energy dissipated by the experimental system is equivalent to the energy input to the experimental system and can be derived by integrating force with respect to displacement. With the available measurements, the dissipated energy can be calculated as the product of the active mass (2Mg) and the integral of the excitation acceleration multiplied by the response velocity (i.e. the differential of the sway with respect to time) with respect to time.

Fig. 7a charts the gradual increase in dissipated energy during select earthquakes from each test series. In this plot, negative gradients relate to the short periods when the shaking table moves in phase with the sway and works to remove energy from the frame. The figure shows that energy dissipation increases from D1 through D18 with F1 dissipating the greatest amount of energy. Fig. 7b presents the dissipated energy normalised by cumulative sway and reveals the effectiveness of the device as an energy dissipator. With the least amount of energy dissipated per unit sway, the low damping of the pre-retrofitted frame is apparent. O series tests are recorded as dissipating nearly double the energy of the pre-retrofitted frame. The first seven D series tests dissipate a greater or equivalent amount of energy to that dissipated in Test D1. When cracks first appear in the web, the device is working at around 60% of its original dissipation capacity. It is interesting to note that small gains in dissipation are observed during the final four D series tests (D15-D18), a trend that may be associated with strain hardening of the box.

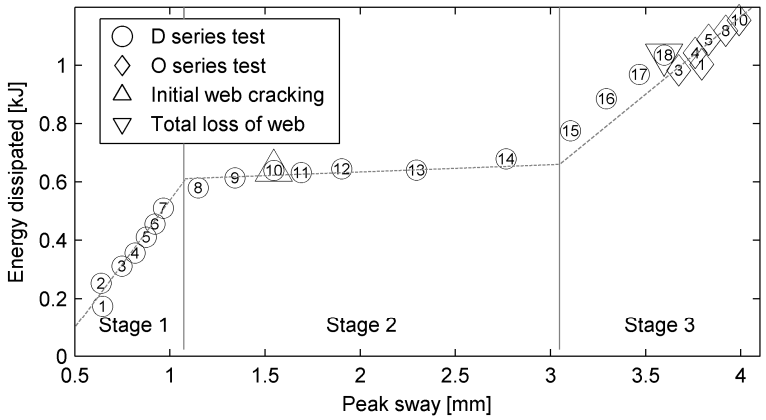

Figure 8. The three tiered lifecycle of the device as determined by seismic loading.

Fatigue lifecycle

Energy considerations also provide supporting evidence for the three-tiered device lifecycle model proposed by Ojaghi et al. (2008). Fig. 7 shows the relationship between cumulative expended energy and peak sway and unifies the trends exhibited during D and O series tests. Three clearly defined stages are evident in the figure. During the first stage, peak sway increases slowly with expended energy and the dissipation per unit sway is greater or equal to that recorded during the initial test. As suggested by Ojaghi et al. (2008), crack initiation marks the transition to the second stage in the device lifecycle and brings about rapid increase in sway. The second stage is short lived, however, and appears to come to an end sometime before the subjective judgement is made that crack propagation is complete. Interestingly, the trend for O series tests can be back-extrapolated to fit the final four D series tests. This suggests that the dissipative ability of the device becomes dominated by the capability of its box section somewhat sooner than expected. During the final stage in the device lifecycle the rate of increase in peak sway is much reduced from Stage 2 but nevertheless remains above that recorded during the initial stage.

The relationship between cumulative dissipated energy and cumulative sway is presented in Fig. 9a. Compared to O series tests, the additional dissipation and degradation of the webbed device is once again evident. Finally, and by way of contrast, the cumulative energy dissipated by a 2mm webbed device during constant strain amplitude test (Fig. 2) has been evaluated (as the integral of the absolute force with respect to absolute displacement) and is presented as Fig. 9b. Quantitative agreement between the energy dissipated during constant strain amplitude tests and that dissipated during variable strain amplitude seismic tests is neither noted nor expected. Nevertheless, the qualitative agreement between the test types is remarkably consistent suggesting again that the dissipation within the shaking table tests is primarily associated with the device.

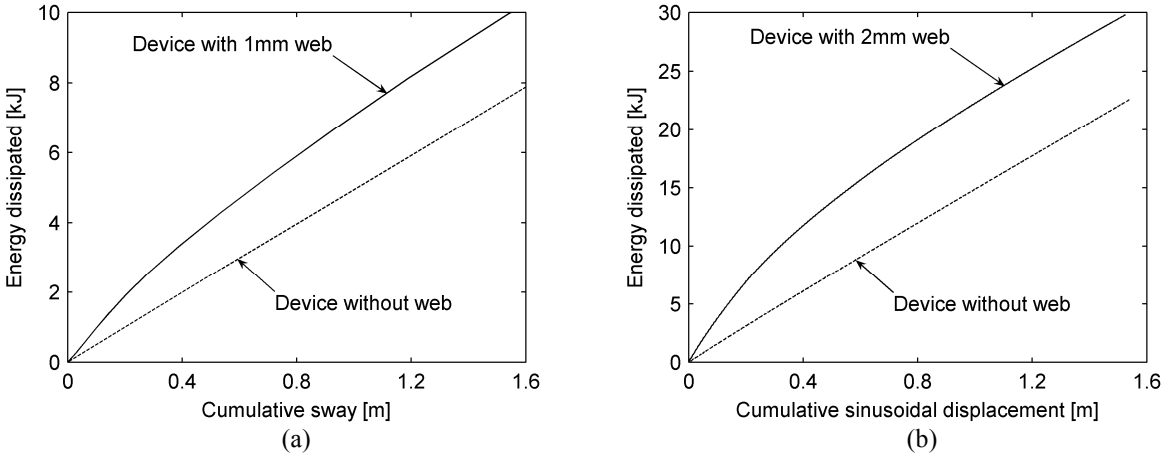

Figure 9. The relationship between dissipated energy and cumulative displacement for (a) shaking table and (b) constant strain amplitude testing.

Conclusions

A shaking table has been used to test the coaction of two passive seismic protection technologies under realistic loading conditions. It is found that a metallic shear-panel dissipative device can effectively be used to prevent the occurrence of potentially damaging levels of seismic sway within a nonlinear-elastic post tension tendon frame. The resilience of the device to the test conditions suggests that it would be effective during a main earthquake event and any aftershocks. Moreover, direct observation reveals that the re-centring capability of the frame is sufficient to remove any residual device offset. Thus, the protection strategies are judged to be complementary. The fatigue life of the system has been investigated by repeat testing. Energy considerations provides experimental evidence that supports a three-tiered lifecycle model and reveal a similar fatigue response as that exhibited during standalone device testing using a constant strain-amplitude test rig.

Acknowledgments

This work was supported by EPRSC, through grant EP/D080088/1.

References

Garlock M.M., Ricles J.M. and Sause R. (2005), Experimental studies of full-scale post-tensioned steel connections, *Journal of Structural Engineering-Asce,* **131(3),** 438-448.

Harris H.G., Sabnis G.M., White R.N. and Mirza M.S. (1999), Structural Modelling and Experimental Techniques, CRC Press, Boca Raton, FL.

Newcombe M.P., Pampanin S., Buchanan A. and Palermo A. (2008), Section analysis and cyclic behaviour of post-tensioned jointed ductile connections for multi-story timber buildings, *Journal of Earthquake Engineering,* **12(**83-110.

Oddbjornsson O., Alexander N.A., Taylor C.A. and Sigbjornsson R. (2008), Shaking Table Testing of Nonlinear Elastic Moment Resisting Frames, *14th World Conference on Earthquake Engineering*, 14WCEE.

Oddbjornsson O. (2009), Dynamics of nonlinear elastic moment resisting frames, *PhD thesis*, University of Bristol, Bristol.

Ojaghi, M., Williams, M.S. and Blakeborough, A. (2008), Development of Energy Dissipating Devices Using Real Time Hybrid Testing, *14th World Conference on Earthquake Engineering*, 14WCEE.

Palermo A., Pampanin S. and Calvi G.M. (2005), Concept and development of hybrid solutions for seismic resistant bridge systems, *Journal of Earthquake Engineering,* **9(6),** 899-921.

Priestley M.J.N. (1991), Overview of PRESSS Research Program, *Pci Journal,* **36(4),** 50-57.

Priestley M.J.N. (2002), Direct displacement-based design of precast/prestressed concrete buildings, *Pci Journal,* **47(6),** 66-79.

Ricles J.M., Sause R., Garlock M.M. and Zhao C. (2001), Post-tensioned seismic-resistant connections for steel frames, *Journal of Structural Engineering-Asce,* **127(2),** 113-121.

Schmidt K., Dorka U., Taucer F., and G. Magnonette, 2004. Seismic retrofit of a steel frame and an RC frame with HYDE systems, *Report of Institute for the Protection and the Security of the* Citizen, European Laboratory for Structural Assessment, EC Joint Research Centre.

Soong, T.T. and G.F. Dargush, 1997. *Passive Energy Dissipation Systems in Structural Engineering*, John Wiley & Sons Ltd, Chichester, England.

Stanton J. and Nakaki S. (2002), Precast Seismic Structural Systems PRESSS Vol. 3-09: Design guidelines for precast concrete seismic structural systems, University of Washington, Seattle.